Available online at www.sciencedirect.com
SCIENCE DIRECT
Journal of the European Ceramic Society 26 (2006) 1043–1049
www.elsevier.com/locate/jeurceramsoc

Solar experimental methods for observing melting plateaux and associated temperature measurements for refractory oxides from 2000 to 3000 °C

D. Hernandez *, G. Olalde

Institut de Science et de Génie des Matériaux et Procédés (IMP-CNRS), BP 5, Odeillo, 66125 Font-Romeu Cedex, France

Received 10 September 2004; received in revised form 1 December 2004; accepted 5 December 2004
Available online 19 February 2005

Abstract

Melting points of refractory oxides at high temperature can be obtained through different techniques (resistive furnaces, induction furnaces, laser beams, imaging furnaces . . .). Here, we present a solar furnace experimental setup and methods developed at the Odeillo Solar Furnace (IMP-CNRS) and used to measure melting and freezing plateau temperatures between 2000 and 3000 °C.

We detail a new procedure we have developed that produces a controllable, long duration temperature plateau, and we discuss the appropriate temperature measurement method.

The principle is to heat a self-crucible product with the solar concentrated flux and to preserve the thermal equilibrium at the melting point temperature by providing a continuously regulated solar flux supply. Two critical points are treated: the control of the right level of temperature and its measurement, which is hampered by the solar reflection.

Results obtained with Al_2O_3 (melting point = 2053 °C) are presented as example.

Keywords: Melting point; Al_2O_3; Thermal properties; Solar Furnace

1. Introduction

The first determinations of the melting points for refractory oxides were published in 1910[1] and 1930[2] and, after an interruption, further work was conducted from 1950.[3] To obtain the melting of the oxides, the means of heating have evolved with technology: from oxyacetylene torches, resistive furnaces, induction furnaces and imaging furnaces to power laser beams. The use of a concentrating solar furnace as radiative heat source appeared in 1960.[4]

The present work belongs to this last field. In parallel with the researches devoted to metal–carbon eutectic fixed points in several National Metrology Institutes,[5] we have evaluated the application of a solar furnace to study the suitability of metal oxide phase changes to be used as secondary reference points,[6] on the International Temperature Scale (ITS-90), in the range 2000–3000 °C.

Preliminary results[7] are promising; they incorporate contamination-free melting and the production of the desired freezing phenomena. They are not yet optimal however, and we wish to increase the duration of the freezing plateau and to improve the temperature measurement method. The goal of the work presented here was to improve these two points.

In the first part of this paper, we describe the experimental installation and we detail the observation technique for the initial melting point observation. In the second part, we present the new method and analysis of the optical temperature measurement in the presence of parasitic reflected solar flux. In both cases, we chose alumina to illustrate the experimental results.

2. Experimental set-up and previous method

The experimental set-up and the method for freezing plateau method observation considered here has been devel-

* Corresponding author.
E-mail address: danielh@imp.cnrs.fr (D. Hernandez).

0955-2219/$ – see front matter © 2005 Elsevier Ltd. All rights reserved.
doi:10.1016/j.jeurceramsoc.2004.12.027

oped at our Institute for related applications.[4] Both have been recently improved for the purpose of producing a secondary reference point.[7]

To avoid contamination, possible alternatives would be to use the self-crucible technique with a radiative heat source such as a concentrating solar furnace, an imaging arc furnace, or a laser, to reach temperatures above 2000 °C. The radiative heat flux must be around 10 MW/m^2 to melt the material under investigation.

2.1. Solar furnace facility

As illustrated in Fig. 1, our solar facility consists primarily of a 2 m diameter fixed, horizontal axis parabolic mirror (3) with a focal length of 0.85 m. The mirror has an aperture of about 0.2 m in diameter at its center, resulting in a 9°-shadowed cone on its axis. The maximum possible incidence angle is 60°.

The solar beam is reflected to the parabola by a 3 m × 3 m heliostat (6). The incident flux on the parabola can be regulated by means of a primary shutter (8) in the path of the parallel solar beam (9), between the heliostat and the concentrator.

With this facility, an average flux of about 14 MW/m^2 can be obtained over a circle of 0.01 m in diameter, which corresponds to a concentration ratio, C_p, of 14,000.

The experimental device, in this case a rotating cylindrical reactor (1) detailed in Fig. 2, is located at the focus of the concentrator.

The concentrated solar flux (2) can be rapidly and completely switched off by a small water-cooled shutter (5) located on a fast-moving mechanism. This movable shutter, which we will refer to as a moving mask, is designed to eliminate the flux in less than 0.1 s. Moreover, it is large enough to cut all the concentrated flux, and features a central hole corresponding to the non-irradiated solid angle of the 0.2 m parabola aperture. These devices allow measurement without solar radiation, which can have a hampering effect.

The optical pyrometers are located behind the parabola (4) and are focused at normal incidence toward the sample. The measurement distance is about 1 m.

The concentrated solar flux is sufficient to melt the refractory oxides easily; generally times of less than 1 min are required. Steady state conditions are reached after only 1 or 2 min; this should be noted as an important asset of the method The primary shutter and moving mask allow the freezing process to be rapidly started and precisely controlled.

2.2. Melting reactor and formation of self-crucible

The cell containing the material is a water-cooled rotating reactor with a cylindrical geometry (diameter D = 0.03 m,

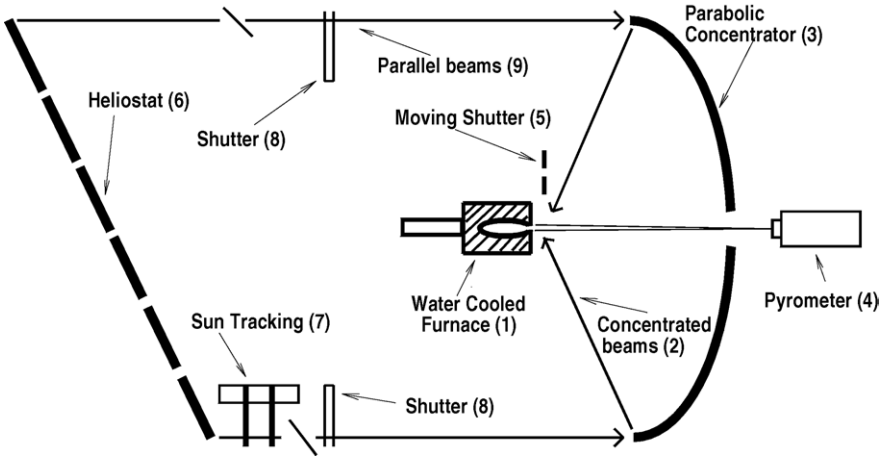

Fig. 1. Schematic diagram of the experimental set-up.

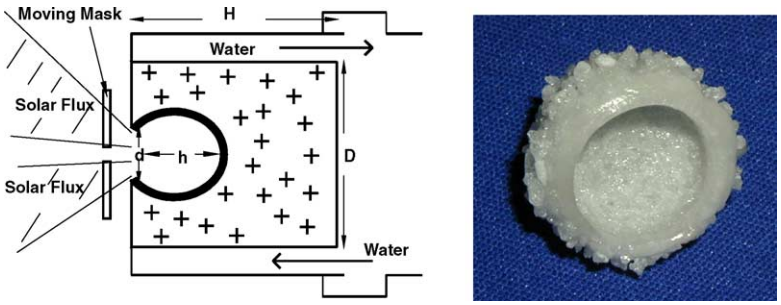

Fig. 2. Rotating reactor for alumina and photo of a cavity.

length $H = 0.04$ m), and an aperture $d = 0.014$ m in diameter (Fig. 2).

The rotational velocity is regulated between 0 and 1200 rpm. The refractory oxides, first in pure extremely fine powder (<50 μm), are preliminary melted to produce larger pellets, which are then ground to obtain a densitified product. The interior of the reactor is then packed with this granular material.

Contamination of the powder in the cavity is prevented by water-cooling the reactor walls and thereby limiting the temperature at the interface between the material and the wall.

When the concentrated solar flux from the parabola is focused on the aperture of the cell, the product starts to melt. Because of the reactor rotation, a cavity characterized by diameter d and a length h, progressively develops until it reaches thermal equilibrium. A self-crucible with a melted inner side surrounded by partially melted pellets is thus obtained. In our case, the resulting dimensions are $d = 1$ cm and $h = 1.5$ cm.

The contamination of the melted product is avoided by the use of the self-crucible (the same material exists on both sides of the liquid–solid interface), the use of non-pollutant radiative heat source and by water-cooling the reactor walls.

2.3. Previous method for the temperature plateau measurements

The temperatures of the melted oxides are measured with radiation thermometers located in the central aperture of the concentrator (Fig. 1). To observe the freezing phenomenon and the temperature plateau, the moving mask is rapidly placed in front of the cavity. Under these conditions, temperatures are measured without the solar reflection contribution. Fig. 3 gives an example of a temperature recorded during an alumina-freezing plateau using a 1.6 μm optical pyrometer.

When the flux is shut down the following features are observed on the temperature history: an abrupt step from level 1, a first cooling in the liquid phase (2), the freezing plateau at $2030 \pm 5\,^{\circ}$C (3) and a second cooling in solid phase (4). The temperature value 2053 °C reported by International Temperature Scale of 1990 is considered as a real temperature.

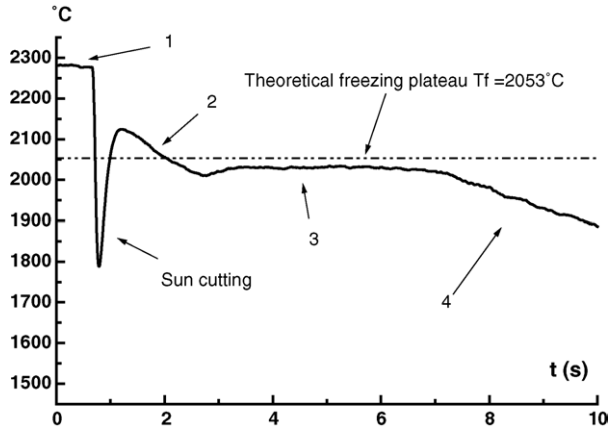

Fig. 3. Example of freezing plateau measurements for Al_2O_3 at 1.6 μm.

The difference between measured and theoretical values of temperature is due to the material emissivity. Even though the measurements are realized inside a cavity, this cavity does not conform to geometrical black body conditions. Typically the cavities have a ratio $h/d = 1.5$ cm/1 cm thus according to Eq. (1) below from,[8]

$$\varepsilon_c = \frac{\varepsilon^{\circ}[1 + (1 - \varepsilon^{\circ})(s/S - \sin^2(\omega)]}{\varepsilon^{\circ}(1 - s/S) + s/S} \quad (1)$$

where ε° is the product's emissivity in the normal direction; ε_c the emissivity of the cavity; ω the half solid angle of the surface aperture; S the cavity surface; and s is aperture surface.

The self-crucible is not deep enough to be a black body if $\varepsilon < 0.9$.

However, the phenomenon is observed through radiance temperature measurements. The freezing plateau appears clearly and stable enough with a characteristic Al_2O_3 super cooling. It lasts only a few (between 2 and 5 s) seconds, the time corresponding to the duration of the transformation of the melted oxide to its solid phase.

3. Method developed to obtain controlled duration plateaus

After considerable work with this system, we concluded that it was necessary to increase the duration of the freezing plateau to have improved temperature measurement.

With the previous method the duration of the plateau is governed by the melted product mass.

To obtain plateaux with a controlled duration we have chosen to work at the thermal equilibrium corresponding to Eq. (2) below (the convection is neglected):

$$\Phi_S = \Phi_R(T_f) + \Phi_C(T_f) \quad (2)$$

where Φ_S is the incident solar flux; Φ_R the radiative flux losses; Φ_C the conductive flux losses; and T_f is melting temperature.

There are two points that need to be solved to make this new method a valid measurement of the freezing point. The first challenge is that the solar flux must be continuously present; thus we must solve the problem of making an optical temperature measurement in the presence of reflected solar radiation. The second challenge is to verify that the true freezing plateau is measured, not a false plateau corresponding to thermal equilibrium. If the temperature observed remains constant under changing flux, we may take this as an indication that the true freezing plateau has been reached.

These two methods are described in detail in Sections 3.1 and 3.2 and they are followed by an analysis of the critical conditions required to produce the desired plateau.

3.1. Apparent spectral radiance of a target heated by a solar concentrator

Despite the existence of several possible pyrometric methodologies, temperature measurement of samples heated at the focus of a solar concentrator have still not received a universal and perfect solution. To underscore the necessary precautions, we present here a short analysis of solar-blind conditions.

In optical pyrometry, the temperature measurement principle is based on the spectral radiance of a black body (used for calibration), and its comparison with the sample's spectral radiance.

For a sample heated at the focus of a solar concentrator, and for a normal-incidence observation, the spectral radiance can be expressed as follows:

$$L^{\circ}(T,\lambda) = \varepsilon^{\circ}(T,\lambda)L_{\mathrm{o}}(T,\lambda) + \int_{\Omega_{\mathrm{p}}} \rho^{\theta,\circ}(T,\lambda,\theta)L_{\mathrm{p}}(\lambda,\theta,\varphi)\cos(\theta)\,\mathrm{d}\Omega_{\mathrm{p}} \quad (3)$$

where L° is the sample's radiance in the normal direction due to solar reflection; L_{o} the blackbody radiance; L_{p} the concentrator's radiance; T the sample's temperature; $\rho^{\theta,\circ}$ the sample's bi-directional reflectivity considered to be independent of φ; λ the wavelength (μm); θ the incident direction from the concentrator to the sample (θ_{M}, θ_{o}: max. and min.); φ the projection of the incident direction θ on a normal plane ($2\pi \geq \varphi \geq 0$); Ω_{p} the solid angle of the concentrator; and $\mathrm{d}\Omega_{\mathrm{p}} = \sin(\theta)\mathrm{d}\theta\mathrm{d}\varphi$ unit solid angle.

Considering that the radiance, $L_{\mathrm{p}}(\lambda, \theta, \varphi)$, of a parabolic concentrator is uniform on its surface, it is possible to relate it to the spectral irradiance at the focus, $E_{\mathrm{p}}(\lambda)$, through:

$$L_{\mathrm{p}}(\lambda) = \frac{E_{\mathrm{p}}(\lambda)}{\pi[\sin^2(\theta_{\mathrm{M}}) - \sin^2(\theta_{\mathrm{o}})]} \quad (4)$$

with

$$E_{\mathrm{p}}(\lambda) = \tau_{\mathrm{a}}(\lambda)R^2(\lambda)C_{\mathrm{p}}E_{\mathrm{o}}(\lambda) \quad (5)$$

where C_{p} is the concentration ratio of the solar concentrator (=14,000 here); E_{o} the extraterrestrial irradiance (1367 W/m^2 at the average sun–earth distance); E_{p} the irradiance at the focus of the concentrator; R the reflectance of a solar furnace component (heliostat or concentrator); and τ_{a} the atmospheric transmittance. The solar extraterrestrial irradiance, $E_{\mathrm{o}}(\lambda)$, is related to its spectral radiance, $L_{\mathrm{s}}(\lambda)$, through:

$$E_{\mathrm{o}}(\lambda) = L_{\mathrm{s}}(\lambda)\Omega_{\mathrm{s}} \quad (6)$$

where L_{s} is the sun radiance and $\Omega_{\mathrm{s}} = 0.71 \times 10^{-4}$ solid angle of the sun (sr).

From Eqs. (3) to (6), the spectral radiance of a sample can finally be expressed as:

$$L^{\circ}(T,\lambda) = \varepsilon^{\circ}(T,\lambda)L_{\mathrm{o}}(T,\lambda) + G_{\mathrm{p}}\tau_{\mathrm{a}}(\lambda)R^2(\lambda)C_{\mathrm{p}}(\lambda)L_{\mathrm{s}}(\lambda)\Omega_{\mathrm{s}} \int_{\Omega_{\mathrm{p}}} \rho^{\theta,\circ}(T,\lambda,\theta)\cos(\theta)\,\mathrm{d}\Omega_{\mathrm{p}} \quad (7)$$

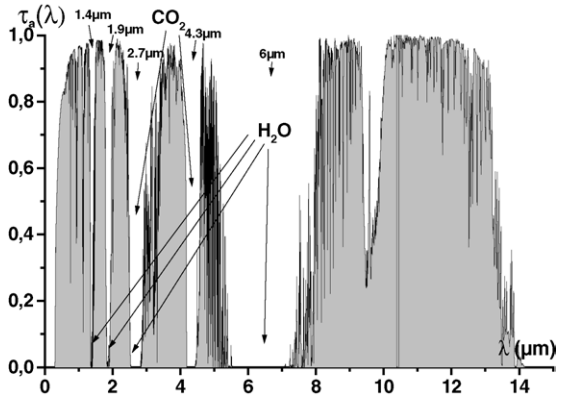

Fig. 4. Atmospheric absorption bands in the infrared spectrum.

where $G_{\mathrm{p}} = 1/\{\pi[\sin^2(\theta_{\mathrm{M}}) - \sin^2(\theta_{\mathrm{o}})]\}$ is a geometric characteristic of the solar concentrator.

It is important to emphasize that the concentration factor also acts as an amplifier for the solar reflection from the sample surface.

To obtain pyrometric measurements without any reflected solar flux contribution, the second term of Eq. (7) must be eliminated. This can be achieved in three different physical ways:

(i) Use the strong absorption bands (Fig. 4) of the atmosphere as a cutting filter to eliminate the solar contribution; this is referred to as "solar blind pyrometry" with $\tau_{\mathrm{a}}(\lambda) = 0$.
(ii) Design the optical components of the solar furnace as a perfect cutting filter, such that $R(\lambda) = 0$.
(iii) Use the blackbody behavior of the sample, so that $\rho^{\Omega_{\mathrm{p}},\circ}(T,\lambda,\theta) = 0$.

These configurations have been previously tested, evaluated and successfully used.[9] In this paper, we limit our examples to measurements in a spectral range 8–12 μm which correspond, for Al_2O_3 (Fig. 5), to the Christiansen region (emissivity = 1) and so to the third condition.

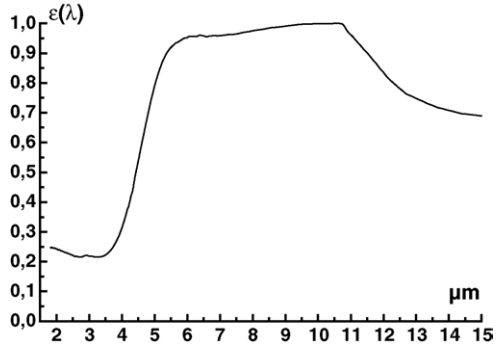

Fig. 5. Measured spectral emissivity ($\varepsilon(\lambda)$) of Al_2O_3 as a function of λ in μm at 2087 °C (after Ref. [10]).

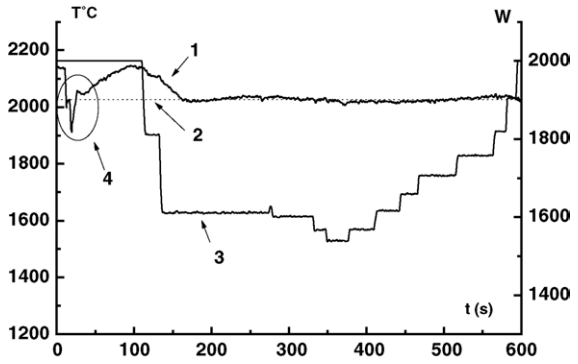

Fig. 6. Example of controlled freezing plateau measurements for Al_2O_3 at 8–12 μm. (1) Self-crucible temperature measurement (°C left axis). (2) Level of the observed plateau (°C left axis). (3) Incident solar flux power (watt right axis). (4) Plateau observed with the cutting solar flux method.

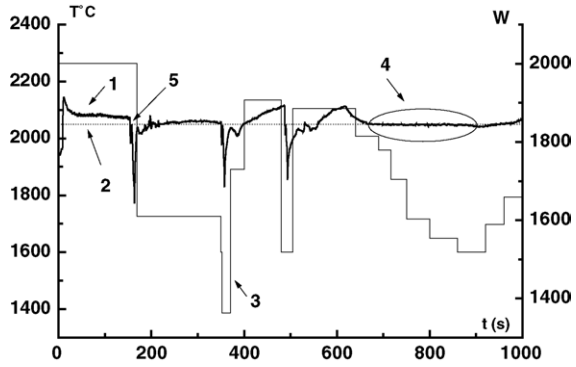

Fig. 8. Example of controlled freezing plateau measurements for Al_2O_3 at 8–12 μm. (1) Self-crucible temperature measurement (°C left axis). (2) Level of the observed plateau (°C left axis). (3) Incident solar flux power (watt right axis). (4) Plateau observed with the cutting solar flux method.

3.2. Method developed for freezing plateau observation at thermal equilibrium

Temperature measurements are achievable with this method if the reflected solar flux problem can be overcome.

Two points have to be determined:

(1) knowledge of the freezing temperature level, and
(2) regulation of the incident solar flux to maintain thermal equilibrium corresponding to Eq. (1).

The first is determined from a preliminary observation of a plateau by using the previous method, completely blocking the solar flux.

The second is worked out by observing the evolution of the ratio $\Delta T(t)/\Delta \Phi_S(t)$: when there is no variation of the temperature at the time that the incident solar flux is changing we conclude that the freezing plateau equilibrium is obtained, liquid mass balancing the cooling or the heating of the material. Figs. 6–8 illustrate these methodologies.

The plateau observed first time in Fig. 6 and curve (1), is shown at higher magnitude in Fig. 7. The plateau duration is only about 3 s. After this operation, the incident solar flux is regulated to approach the registered level of the plateau. Curve (2) gives the value of the incident solar power. After $t = 200$ s, the temperature of the self-crucible is stabilized around a plateau at 2045 ± 15 °C (curve (2)) while the incident flux is increasing on the order of $\Delta \Phi_S = 8.5\%$. The duration of this equilibrium can be maintained as long as required. Fig. 8 presents another example of a controlled duration freezing plateau.

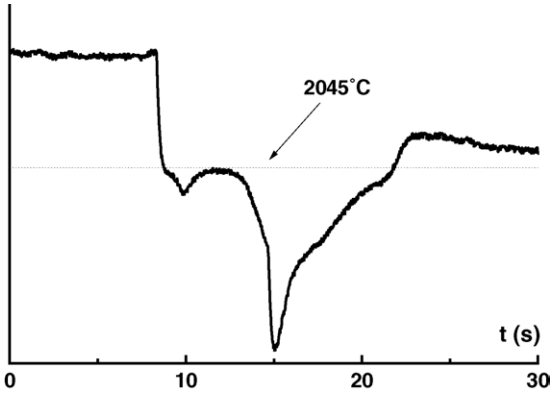

Fig. 7. Higher magnification of self-crucible temperature in Fig. 6, zone 4.

The freezing phenomena plateau is first observed at point 5 in the figure and its level corresponds to the curve (2).

Before $t = 650$ s, the temperature of the self-crucible is dependent on the value of the solar incident flux. It appears that the sample is reaching the plateau between $200\text{ s} < t < 350$ s, but because the solar flux is also constant in this period it is impossible to distinguish between a plateau and thermal equilibrium.

After $t = 650$ s and until $t = 900$ s, the measured temperature is stabilized at 2050 ± 3 °C while the incident flux is decreasing on the order of $\Delta \Phi_S = 15\%$. Here, we can clearly see that a freezing plateau has been established and that the solar reflection does not hamper the temperature measurements.

The validity of the method developed for the freezing plateau observation at the thermal equilibrium is demonstrated through the presented examples.

3.3. Analysis of the observation condition for the thermal equilibrium method

Although it appears that the results obtained with this method unequivocally establish a freezing plateau, it is convenient to detail the conditions necessary to obtain a freezing plateau.

The radiometer located on the horizontal axis of the concentrator characterizes the bottom of the self-crucible. Its observation surface is a disc of 6 mm diameter.

The experiments have shown that for temperature measurements corresponding to a thermal treatment as presented in Figs. 6 and 8, four periods can be distinguished during a cooling from the liquid to the solid state:

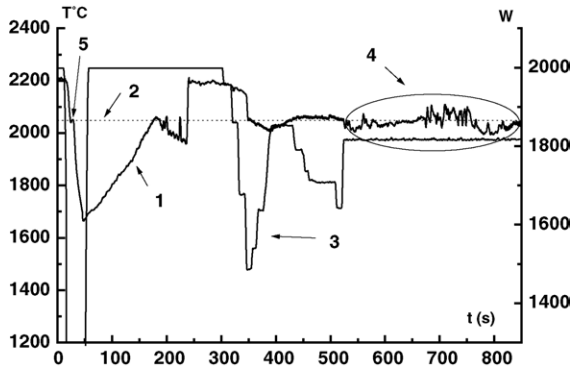

Fig. 9. Example of controlled freezing plateau measurements for Al_2O_3 at 8–12 μm. (1) Self-crucible temperature measurement (°C left axis). (2) Level of the observed plateau (°C left axis). (3) Incident solar flux power (watt right axis). (4) Observed instable plateau. (5) Plateau observed with the cutting solar flux method.

(1) $\Delta T/\Delta \Phi_S = 0$–$0.2$: the mass of the melted product is thick enough to minimize the effect of the solar flux variation.
(2) $\Delta T/\Delta \Phi_S = 0.1$–$0.5$: the volume of the liquid mass has diminished and the surface temperature reacts to a solar flux variation.
(3) $\Delta T/\Delta \Phi_S = 0$: the temperature is governed by the phase law, this is the freezing plateau.
(4) $\Delta T/\Delta \Phi_S = 0.5$–$0.9$: the material is cooling to a solid phase.

The control parameter $\Delta T/\Delta \Phi_S$ has been proven to be the governing parameter for selecting conditions for good measurements.

However, it is important to describe the difficulties relative to the thermal equilibrium. For stable and correct measurements, the target observed by a pyrometer (a 6 mm diameter disk) has to be composed of intimately mixed solid and liquid. This is true for the examples shown in Figs. 6 and 8. When this is not the case, cooled solid or heated liquid disturbs the freezing plateau.

The example presented in Fig. 9 illustrates this phenomena. The freezing temperature had been correctly identified earlier (stage number 5 of the record), but the temperatures observed during stage 4 varied around the plateau level while the incident solar flux was constant, indicating the likely presence of a mixture consisting of large regions of cooled solid material and small volumes of superheated liquid.

The operator thus has the responsibility to conduct the experiment and principally the self-crucible formation carefully to obtain favorable conditions. In the case of the alumina, these are generally obtained for cavities characterized by $h = 1.5d$.

The second point to discuss is the measurement method. With the disturbing influence of solar reflection solved (Section 2), the problems of measuring the true temperatures remain classical: calibration of the radiometer and knowledge of the product emissivity.

These problems underscore the calibration motivation behind our work: the ITS-90 (International Temperature Scale, 1990) does not cover this temperature range and, for us, the accuracy cannot be certified.

The reproducibility appears as the appropriate parameter to evaluate the method reliability. For our experiments during the plateau, it was about 5 °C.

The instability of the measured area due to non-controlled mixing can reach ±15° even if the cavity conditions are favorable.

The emissivity data is difficult to obtain. For alumina, the bibliography offers a large range of emissivity values over the appropriate wavelength range. Taking the freezing temperature equal to 2053 °C, the calculated cavity emissivity corresponding to the pyrometer calibration, is about 0.996 in accord with Eq. (1) and the value given in Fig. 5. When the emissivity of the product is unknown, the operator must choose a solar blind window to eliminate the parasitic reflections. In this case, the measured radiance temperature can vary greatly from the theoretical value. For black body conditions, it is necessary to deploy spectroradiometer measurement to determine the Christiansen wavelength.[10,11]

After this critical analysis, we can conclude that the method described if carefully done is a valid mean to obtain controlled freezing plateaux.

4. Conclusions

The work presented here confirms the capability of a solar technique to obtain freezing plateaux for refractory oxides.

Although others have presented similar results using measurements taken during a freezing plateau obtained with the solar flux completely eliminated by some type of shutter device, our work presents the first example of measurements taken during a freezing plateau with controlled duration obtained under conditions of carefully controlled solar flux.

The study of the materials' monochromatic radiative properties appears as a fundamental complementary approach. Measurements at the Christiansen region,[10,11] which is generally present in polar dielectric materials and more particularly in dielectric oxide materials, would offer black body conditions and so improve reproducibility.

A special metrological approach has to be implemented to achieve the determination of the melt–freeze temperatures with a clear traceability to ITS-90.

At this time, it can be concluded that the method proposed here has merit and offers potential for accurate measurement of high-temperature melting processes up to about 3000 °C.

Acknowledgements

The Bureau National de Métrologie (B.N.M.) is gratefully acknowledged for its scientific and financial support.

We thank Christophe Palau for his participation to the experimentations.

References

1. Ruff, O. and Goecke, O., Uber das Schelmelzen und Verdampfen unserer sogenannten hochfeuerfesten Stoffe. *Z. Angew. Chem.*, 1911, **24**, 1459.
2. Wartenberg, H. and Werth, H., Schmelzdiagramme höchstfeurfester Oxyde. *Z. Anorg. Chem.*, 1930, **190**, 178.
3. Schneider, S. J., Compilation of the melting points of the metal oxides. *Nat. Bur. Stand. Monog.*, 1963, **68**, 31.
4. Foex, M., Mesure des points de solidification des oxydes réfractaires. *Rev. Int. Htes Temp. Réfract.*, 1966, **3**, 309–326.
5. Yamada, Y., Sakate, H., Sakuma, F. and Ono, A., Short Communication–Radiometric observation of melting and freezing plateaus for a series of metal-carbon eutectic points in the range 1330 °C to 1950 °C. *Metrologia*, 1999, **36**(3), 206–209.
6. Bedford, R. E., Bonnier, G., Maas, H. and Pavese, F., Recommended values of temperature on the International Temperature Scale of 1990 for a selected set of secondary reference points. *Metrologia*, 1996, **33**, 133–154.
7. Hernandez, D., Olalde, G., Bonnier, G., Le Frious, F. and Sadli, M., Evaluation of solar furnace application to study the ability of metal oxides to be used as secondary reference points in the range 2000–3000 °C. *Measurements*, 2003, **34**, 101–109.
8. Gouffé, A., *Transmission de la chaleur par Rayonnement, Cahier 1*. Eyrolles, 1978.
9. Hernandez, D., Olalde, G., Gineste, J. M. and Gueymard, C., Analysis and experimental results of solar-blind temperature measurements in solar furnaces. *J. Solar Energy Eng.*, 2004, **126**, 645–653.
10. Rozenbaum, O., De Sousa Meneses, D., Auger, Y., Chermanne, S. and Echegut, P., A spectroscopic method to measure the spectral emissivity of semi-transparent materials up to high temperature. *Rev. Sci. Instrum.*, 1999, **70**(10), 4020–4025.
11. Markaham, J. R., Best, P. E., Solomon, P. R. and Yu, Z. Z., Measurement of radiative properties of ash and slag by FT-IR emission and reflection spectroscopy. *Trans. ASME J. Heat Transfer*, 1992, **114**, 458–464.